Reprinted from The Journal of Physical Chemistry, 1992, 96.

Structure of Monolayers Formed by Coadsorption of Two *n*-Alkanethiols of Different Chain Lengths on Gold and Its Relation to Wetting[1]

Paul E. Laibinis,[†] Ralph G. Nuzzo,*[,‡] and George M. Whitesides*[,†]

Department of Chemistry, Harvard University, Cambridge, Massachusetts 02138, and Departments of Materials Science and Engineering and Chemistry, University of Illinois at Urbana-Champaign, Urbana, Illinois 61801 *(Received: February 5, 1992)*

We have characterized and correlated the structure and wetting properties of self-assembled monolayers (SAMs) on gold derived from two different mixtures of *n*-alkanethiols ($C_{12}SH$ and $C_{18}SH$; $C_{12}SH$ and $C_{22}SH$); in each of these SAMs, one thiol had a perdeuterated alkyl chain and one a perprotonated chain to allow the two alkanethiols to be distinguished in the SAM by polarized infrared external reflectance spectroscopy (PIERS). The hydrocarbon parts of the SAMs consist of well-defined regions exhibiting structural characteristics reminiscent of those formed in crystalline and liquidlike states. In each SAM, both the shorter alkanethiolate and the section of the longer alkanethiolate closest to the gold contain very low densities of gauche conformations (and presumably are ordered) over all compositions of the SAM. The terminal portion of the longer alkanethiolate—that which extends beyond the terminus of the shorter alkanethiolate—is disordered. The density of gauche conformers present in this component decreases as its concentration in the SAM is increased. The advancing and receding contact angles (θ_a and θ_r, respectively) of water and hexadecane (HD) respond differently to the disordered region: for hexadecane, θ_a(HD) and θ_r(HD) reach minima when the interface is present in the disordered, liquidlike state; for water, $\theta_a(H_2O)$ and $\theta_r(H_2O)$ appear insensitive to the presence of this disorder. The IR spectra of these mixed SAMs are consistent with previous inferences from wetting that the components of the SAMs, *as prepared here* (adsorption of 1 mM thiol from ethanolic solutions over 24–48 h at ~25 °C), do not phase segregate into macroscopic islands. The larger interpretation which follows from the data, however, is that this result reflects a structural architecture derived from a kinetically controlled growth process. Under suitable conditions, phase segregation is important as might be expected from consideration of elementary thermodynamics. The importance of kinetic and thermodynamic factors in the structural characteristics of multicomponent SAMs is discussed.

Introduction

Multicomponent self-assembled monolayers (SAMs) derived from the adsorption of organosulfur compounds on gold are useful in fundamental studies of wetting,[2,3] adhesion,[4,5] and electron transfer,[6,7] and may also provide elements for the fabrication of molecular-based devices and sensors.[8,9] While single-component SAMs on gold[10-16] and other metal surfaces[17-21] have been characterized structurally in detail, analogous studies on SAMs derived from more than one adsorbate have yet to be reported. This paper examines the phase properties and structure of SAMs on gold derived from the exposure of the substrate to various mixtures of *n*-alkanethiols of different chain lengths—$C_{12}SH$ and $C_{18}SH$, $C_{12}SH$ and $C_{22}SH$—and relates the structural properties (inferred primarily from data obtained using infrared spectroscopy) to a macroscopic property, namely, wetting.

n-Alkanethiols ($HS(CH_2)_nX$) adsorb from solution onto gold surfaces and form densely packed, oriented monolayer films with the sulfur bound to the gold as a thiolate (Au_n-Au(I)$^-$SR) and the tail group X exposed at the monolayer/air(liquid) interface.[2-8,10-16,22-25] The substrates we employed most routinely are polycrystalline films having a strong (111) texture.[20,23,24,26] The sulfur atoms are bonded to this lattice in an ordered $(\sqrt{3}\times\sqrt{3})R30°$ overlayer.[12-15] Monolayers composed of more than one alkanethiolate can be formed by exposing a gold surface to solutions containing mixtures of alkanethiols.[2-8,25,27-29] The surface composition of the resulting "mixed" monolayer is, in general, different from but parallel to the composition of the solution from which it was formed.[2-4,7,25,27-29] The coadsorption of thiols thus provides a general method for generating monolayer films expressing varied molecular textures at the interface (by varying the chain lengths) and interfacial compositions (by varying the terminating functional groups, X).

We have explored mixed monolayers composed of two *n*-alkanethiolates having different chain lengths as models for complex interfaces,[25,27-29] and inferred from the wetting properties of the mixed SAMs that these systems do not phase separate macroscopically. Since wetting is due to short-range interactions (<5 Å),[30-32] we hypothesized that the structure of these mixed SAMs could be thought of as being a disordered hydrocarbon layer supported on a crystalline or liquid-crystalline underlayer:[27-29] that is, we expect that the polymethylene chains projecting beyond the region of the shorter chains may, for appropriate concentrations of coadsorbates, contain densities of gauche conformations comparable to those in liquid phases (Figure 1).[33]

In this study, we examined mixed SAMs comprising two *n*-alkanethiolates having different chain lengths; one had a perdeuterated alkyl chain to allow the two components to be distinguished spectroscopically. Chain lengths were chosen based on both the results obtained in previous studies[27-29] and on the commercial availability of precursors (perdeuterated alkyl bromides) for the synthesis of the thiols. We characterized the structure of the components in the SAM using infrared spectroscopy. Vibrational spectroscopy is an invaluable tool for defining the structure of monolayers.[10,11,16-21] In earlier studies, we have shown that the alkyl chains of thiolate monolayers supported on gold formed a canted phase which can be described well by an average orientation of a single, all-trans chain having a tilt of ~27° relative to the surface normal.[11b,20] The value determined by infrared spectroscopy is compatible with values obtained by diffraction methods.[12,13,34] This value originates from the formation of a commensurate lattice of thiolates on the gold surface, $(\sqrt{3}\times\sqrt{3})R30°$, that yields a greater area per thiolate (21.4 Å^2)[12] than the cross-sectional area of an alkyl chain (18.4 Å^2).[35] As a result, the chains tilt to maximize their van der Waals interaction.[36] For the mixed systems studied here, macroscopic phase separation of the two components would lead to domains in which each component has the average structure found in pure SAMs (Figure 1a). Smaller degrees of mixing should yield SAMs where the tails of the longer *n*-alkanethiolate must adopt more complex conformations (and perhaps tilt further away from the surface normal) to achieve van der Waals interaction, and the chain groups in the near-surface region should be less ordered than the alkyl chains are in pure SAMs (Figure 1b,c). In general, we expect that the highest gauche densities per long chain will exist in those phases in which the value of its mole fraction are lowest and, most

[†] Harvard University.
[‡] University of Illinois at Urbana-Champaign.

0022-3654/92/2096-5097$03.00/0

TABLE I: C–H and C–D Stretching for Polycrystalline Alkyl Chains[a]

mode description[b]	abbrevn	peak frequency, cm⁻¹ C–H	C–D	direction of transition dipole moment in molecular coordinates
methyl asym (ip)	r_a^-	2964	2224, 2219	∥ CCC backbone, ⊥ C–CH_3 bond
methyl asym (op)	r_b^-	2954	2210	⊥ CCC backbone plane
methyl sym	r^+ (FRC)	2935	2123, 2118	∥ C–CH_3 bond
methylene asym	d^- (α)	2925		⊥ CCC backbone plane
methylene asym	d^-	2918[c]	~2195	⊥ CCC backbone plane
methylene sym	d^+ (FRC)	2894		∥ CCC backbone plane, ip HCH plane
methyl sym	r^+	2879	2073	∥ C–CH_3 bond
methylene asym	d^+ (α)	2853		∥ CCC backbone plane, ip HCH plane
methylene sym	d^+	2850	~2098	∥ CCC backbone plane, ip HCH plane

[a] Based on data taken from refs 17, 20, 24, 37, and 38 for dialkyl disulfides, alkanoic acids, and alkanes. [b] Abbreviations used: asym = asymmetric or antisymmetric, sym = symmetric, ip = in plane, op = out of plane, FRC = Fermi resonance splitting component, α = CH_2 groups located at either end of the alkyl chain, ∥ = parallel, ⊥ = perpendicular. [c] MacPhail et al.[38] have reported a frequency for d^- of 2915 cm⁻¹ for an orthorhombic crystalline sample of n-$C_{21}H_{44}$ at T < 10 K.

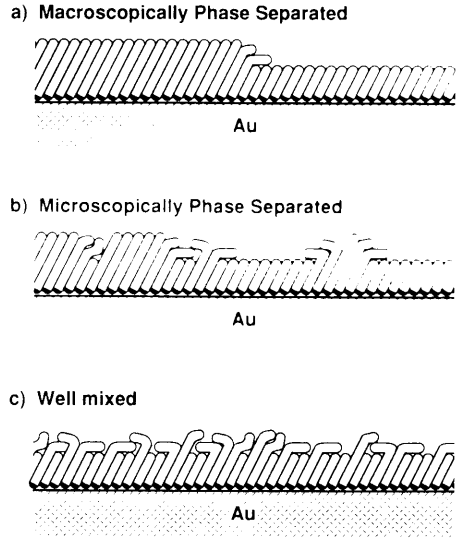

Figure 1. Schematic illustrations of mixed SAMs on gold derived from mixtures of n-$C_{12}H_{25}SH$ and n-$C_{22}H_{45}SH$.

importantly, that these conformers will be inhomogeneously distributed along its length. This study determined, using PIERS, the relative density of gauche bonds in protonated alkyl chains (C_{12} and C_{22}) incorporated into mixed SAMs with perdeuterated chains, and used the resulting information to infer details of mixing of the chains, and of order, as a function of the composition of the SAMs.

Results

SAMs Prepared from Ethanolic Solutions Containing Mixtures of $C_{12}D_{25}SH$ and $C_{22}H_{45}SH$. Figure 2 displays data from ellipsometry, X-ray photoelectron spectroscopy (XPS), and wetting by water and hexadecane (HD) for SAMs derived from ethanolic solutions containing mixtures of n-$C_{12}D_{25}SH$ and n-$C_{22}H_{45}SH$ (total thiol concentration = 1 mM); similar data on related systems have been discussed in detail elsewhere.[28,29] The vertical line in Figure 2 marks the solution composition required to form a SAM having an equimolar composition of the two adsorbates. This SAM exhibited the lowest receding value ($\theta_r(H_2O)$) and the highest hysteresis ($\Delta \cos\theta = \cos\theta_r - \cos\theta_a$) in the contact angles of water.

SAMs derived from these solutions were characterized by infrared spectroscopy (Figure 3). Spectra of the C–H and C–D stretching regions (2800–3050 and 2000–2300 cm⁻¹, respectively) were obtained; monocomponent SAMs derived from pure samples of n-$C_{12}D_{25}SH$ and n-$C_{22}H_{45}SH$, respectively, were used as the spectral references. Mode assignments are given in Table I.[17,20,24,37,38]

The position and width of peaks in the C–H stretching region change with surface composition. The d^+ and d^- modes of the

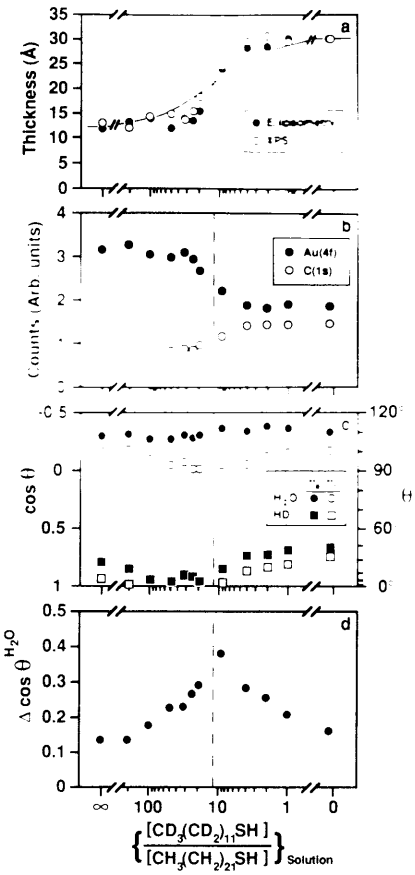

Figure 2. Ellipsometry, XPS, and wetting data for SAMs on gold derived from ethanolic solutions containing mixtures of $HS(CD_2)_{11}CD_3$ and $HS(CH_2)_{21}CH_3$. (a) Thickness of the SAMs determined by ellipsometry and XPS. Thicknesses determined from XPS were calibrated to the ellipsometric thickness of a SAM derived from $HS(CH_2)_{21}CH_3$ (see Experimental Section). The solid line represents the thicknesses expected if the surface compositions directly paralleled the solution compositions. Ellipsometric thickness are estimated to be ±2 Å; thicknesses determined by XPS are estimated to be ±1 Å. (b) XPS intensities of the Au(4f) and C(1s) peaks; values are from single measurements (see Experimental Section) and are estimated to ±5%. (c) Wetting properties of the SAMs: advancing and receding contact angles (θ_a and θ_r, respectively) of water and hexadecane (HD). Errors in θ are ~±3°. (d) Hysteresis ($\Delta \cos\theta = \cos\theta_r - \cos\theta_a$) in wetting by water. The dashed vertical line represents the solution composition required to generate SAMs having an equimolar composition of the two adsorbates as determined by XPS.

CH_2 groups exhibit the largest changes as the SAM incorporates a larger mole fraction of the longer alkanethiol: the peaks shift to lower frequencies and become narrower. For SAMs of intermediate composition, the peaks associated with the d^+ and d^- modes exhibit asymmetry (beyond the asymmetry in d^- due to

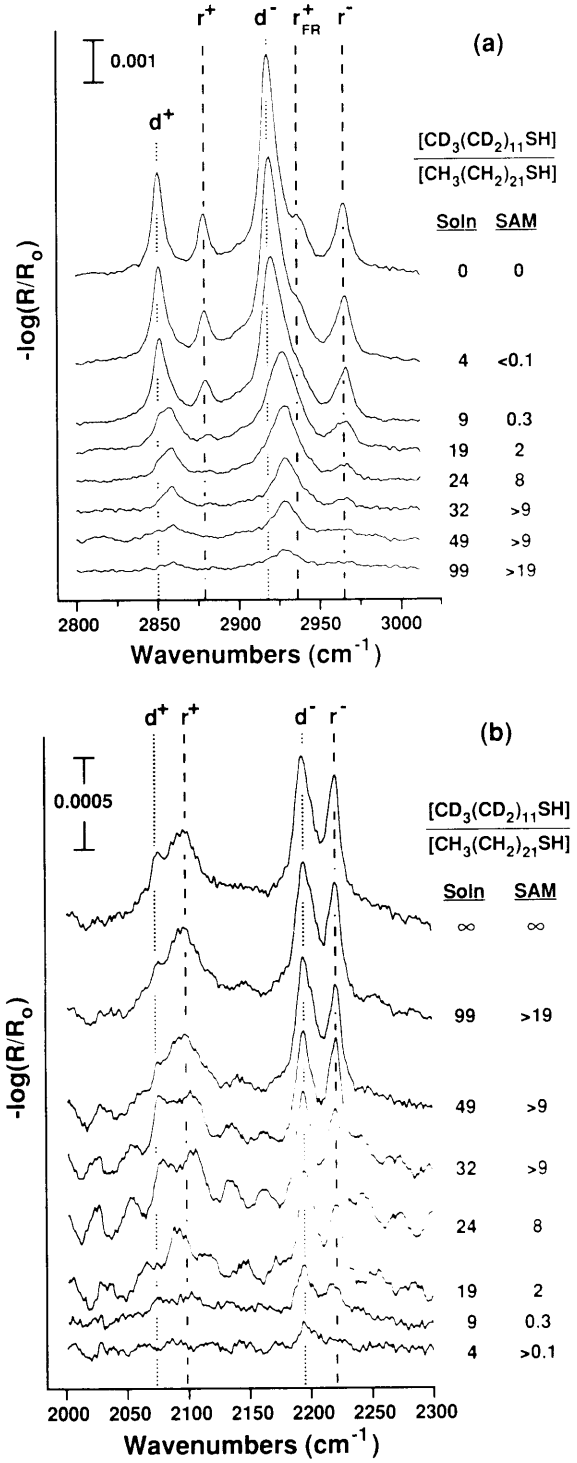

Figure 3. PIERS spectra of SAMs on gold derived from ethanolic solutions containing mixtures of $HS(CD_2)_{11}CD_3$ and $HS(CH_2)_{21}CH_3$. (a) The C–H stretching region. (b) The C–D stretching region. Total thiol concentration ($[C_{12}]_{soln} + [C_{22}]_{soln}$) = 1 mM. The ratios of the two thiolates on the surface ($[C_{12}S]_{SAM}/[C_{22}S]_{SAM}$) were estimated from XPS data; we estimate the error in surface compositions to be ±~5% in the value of $[C_{12}]_{SAM}/([C_{12}]_{SAM} + [C_{22}]_{SAM})$. The dotted and dashed vertical lines correspond to methylene and methyl vibrational modes, respectively. Mode assignments are given in Table I.

the presence of the asymmetric CH_3 Fermi resonance at 2935 cm^{-1}); a shoulder at ~2850 and ~2918 cm^{-1} (frequencies corresponding to d^- and d^+ modes, respectively, in trans-extended alkanes) is observed in these spectra. The line shapes of the d^+ and d^- modes, assigned as the symmetric and asymmetric CH_2 C–H stretching vibrations, respectively, do not conform in these intermediate regimes to those formed in either the liquid or solid state. The asymmetries evident at both high and low frequency, for example, in the d^- mode, are consistent with (but do not independently establish) the coexistence of regimes of high gauche density and of extended trans segments. At low surface concentrations of the longer thiolate, the intensities of the high-frequency components of d^+ and d^- are greater than those at lower frequency (i.e., the crystalline regions). The virtual absence of intensity at 2918 cm^{-1} for those SAMs composed of <10% longer thiolate ($[C_{12}]_{SAM}/[C_{22}]_{SAM} > 9$) suggests that the chain ends of the longer thiolate in the mixed SAMs may be completely disordered. This inference follows from several independent lines of reasoning. First, we have shown in an earlier study[20] that the C–H stretching modes of the alkyl chains are highly coupled. It follows as a result that the intensity of an all-trans C_{22} chain cannot be algebraically scaled to predict that of a shorter chain. It is also likely that the nature of these couplings is sensitive to the conformational states of the chains. We therefore cannot assume that an extended trans segment in a minor chain population can be linearly related via its mole fraction to the intensities found in a homogeneous all-trans reference phase. The d^+ and d^- band intensities for the trans CH_2 populations therefore are likely to decline more rapidly than would be predicted by a simple linear weighting of their content in the SAM. The peak shapes of the d^+ and d^- modes in these spectra also require that the spectral contributions of the methylenes of the gauche segments be, to a similar degree, "abnormally intense". The key insight here is that the structure is not conserved. The "disordered" phases have chain architectures that are distinctly different from the canted phases formed by single-component SAMs. The projections of the transition dipole moments of the C–H stretching vibrations along the surface normal direction[39] are likely to be significantly different (and presumably larger) for many relevant long chain concentrations.

The methyl modes (r^+ and r^-) in the C–H region exhibit no change in frequency with composition. The ratio of the intensities of these two modes (r^+/r^-) in the spectra is approximately the same in the spectra, although our ability to measure the intensity of these modes is limited. This trend is consistent with the belief that the thermal population of chain-end gauche conformers yields a disordered methyl surface projection at room temperature.[11c,13,40] It is unclear from the spectra if the weighting of the r_a^- and r_b^- modes changes with composition.

In Figure 3b, the peaks associated with the C–D stretching modes change in intensity with changes in the ratios of concentrations of thiols in the contacting solutions (and, thus, of the mixed SAMs); the widths and positions of the peaks, however, remain relatively unchanged. Given the quality of our data and the complexity of interpreting C–D stretching frequencies,[17,38] we are hesitant to analyze these data further. The spectra do, however, also provide a useful comparison with spectra given later in the paper.

Figure 4 displays the wetting and IR data of the mixed SAMs relative to their surface composition. The lowest values of θ_a(HD) and θ_r(HD) occur over a range of surface compositions where the longer thiolate is the minor component. Over this range of compositions, the positions of the d^+ and d^- modes suggest that the portions of the longer component contacting the solvent are characterized by considerable disorder. In SAMs that contain higher surface compositions of the longer thiolate, this component is present in a simpler form and the wetting properties of the mixed SAMs by HD resemble those of a low-energy methyl surface.

As we have noted above, the integrated intensities of the d^+ and d^- modes cannot be directly related to the composition of the longer alkanethiolate in the SAM (Figure 4c): at intermediate compositions, the intensity is greater than expected for a simple statistical weighting of the integrated intensity of a pure C_{22} SAM. The intensities of these modes are affected by, among other factors, the details of the mode couplings as well as the orientation of the polymethylene chain. The simplest case arises for orientations of an all-trans chain for which cants of the main chain axis further away from the surface normal become more intense.[39] The deviations in d^+ and d^- evidenced in Figure 4 suggest that the *average* orientation of the chain in the mixed SAMs is greater than the tilt for a pure SAM (~27° from the surface normal); however,

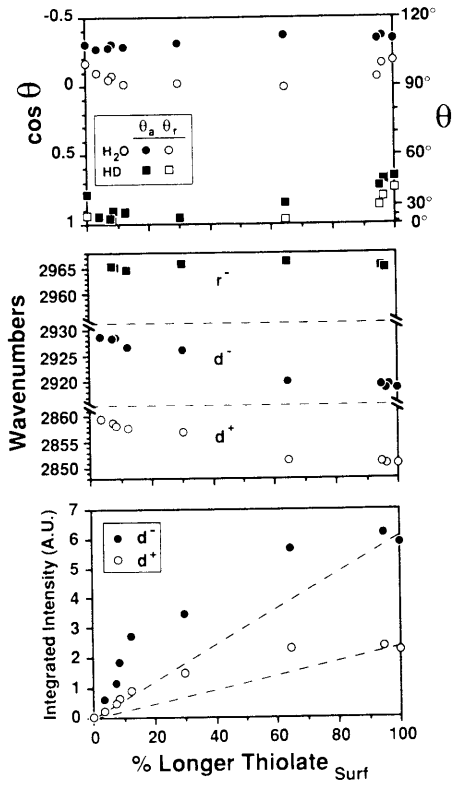

Figure 4. Wetting properties and C–H stretching mode data of SAMs on gold derived from ethanolic solutions containing mixtures of $CD_3(CD_2)_{11}SH$ and $CH_3(CH_2)_{21}SH$. The infrared data are for the longer *n*-alkanethiolates in the mixed SAMs, namely, those elements of the SAM derived from $CH_3(CH_2)_{21}SH$. The compositions of the SAMs were determined by XPS (see Experimental Section); we estimate the error in surface compositions to be ±5% of the *x*-axis. The dashed lines in the lowest panel represent the intensities expected for these modes if the longer alkanethiolate were present in large-domain-size islands (Figure 1a). AU = arbitrary units.

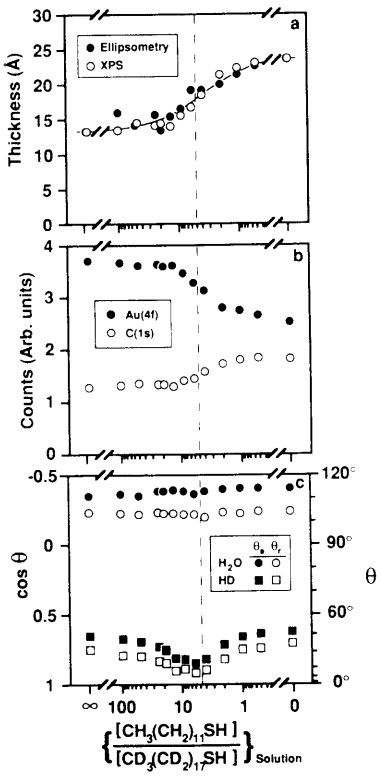

Figure 5. Ellipsometry, XPS, and wetting data for SAMs on gold derived from ethanolic solutions containing mixtures of $HS(CH_2)_{11}CH_3$ and $HS(CD_2)_{17}CD_3$. Data are plotted as in Figure 2. Thicknesses determined from XPS were calibrated to the ellipsometric thickness of a SAM derived from $HS(CH_2)_{11}CH_3$ (see Experimental Section).

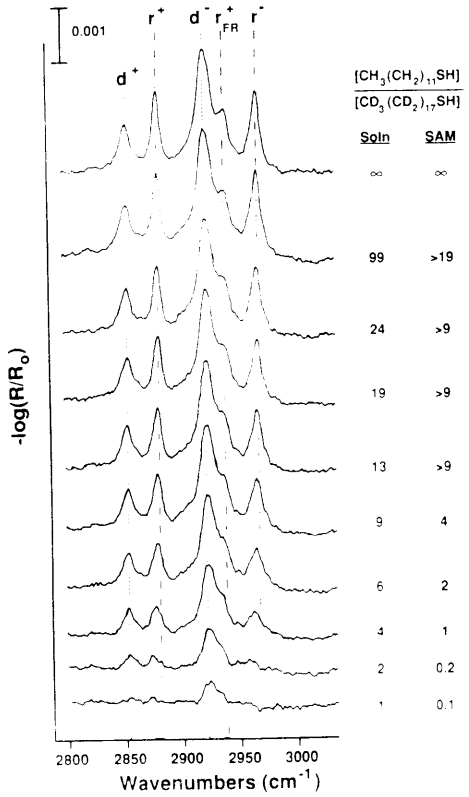

Figure 6. PIERS spectra of SAMs on gold derived from ethanolic solutions containing mixtures of $HS(CH_2)_{11}CH_3$ and $HS(CD_2)_{17}CD_3$. Total thiol concentration ($[C_{12}]_{soln}$ + $[C_{18}]_{soln}$) = 1 mM. The ratios of the two thiolates on the surface ($[C_{12}S]_{SAM}/[C_{18}S]_{SAM}$) were estimated from XPS data; we estimate the error in surface compositions to be ±~5% in the value of $[C_{12}]_{SAM}/([C_{12}]_{SAM} + [C_{18}]_{SAM})$. The dashed and dotted vertical lines correspond to methyl and methylene vibrational modes, respectively. Mode assignments are given in Table I.

because the changes in intensity occur concomitant with changes in the line width and peak frequency of these modes (Figure 3a), the data do not allow a simple picture to be drawn for the longer alkanethiolate. What is clear from these data is that the detailed phase behaviors of the longer chains are responding to the short-chain constituents of the SAM as if *the presence of the shorter alkanethiolate constitutes a significant and varying perturbation of the local molecular environment of the longer alkanethiolate.*

SAMs Prepared from Ethanolic Solutions Containing Mixtures of n-$C_{12}H_{25}SH$ and n-$C_{18}D_{37}SH$. Figure 5 displays the ellipsometric, XPS, and wetting data on SAMs derived from ethanolic solutions containing mixtures of $C_{12}H_{25}SH$ and $C_{18}D_{37}SH$ (total thiol concentration = 1 mM). These experiments are complementary to those in the preceding section. Here, the *shorter* chains are protonated and thus are the more easily analyzed by PIERS. The data are qualitatively similar to those in Figure 2. The differences in wetting between the mixed and pure SAMs are less dramatic than those data summarized in Figure 2c and probably reflect the smaller difference between the chain lengths of the two alkanethiols used (difference = 6 vs 10 carbon atoms).[28]

SAMs derived from these solutions were characterized by infrared spectroscopy (Figure 6). The C–H spectra were obtained using a SAM derived from $C_{18}D_{37}SH$ as a reference; the low intensity of C–D stretching modes relative to C–H modes precluded obtaining spectra of the longer alkanethiolate having useful intensity.[41]

The IR spectra in Figure 6 exhibit trends opposite those observed in Figure 3a. The methylene C–H stretching modes (d^+ and d^-) exhibit little change in position or peak width with decreasing surface composition of the alkanethiol; the methyl C–H stretching modes (r^+ and r^-) change both in width and position. The lack of weighted intensity for the d^+ and d^- modes at higher frequencies (or even large band asymmetries) suggests that the density of gauche conformers in the shorter component of the

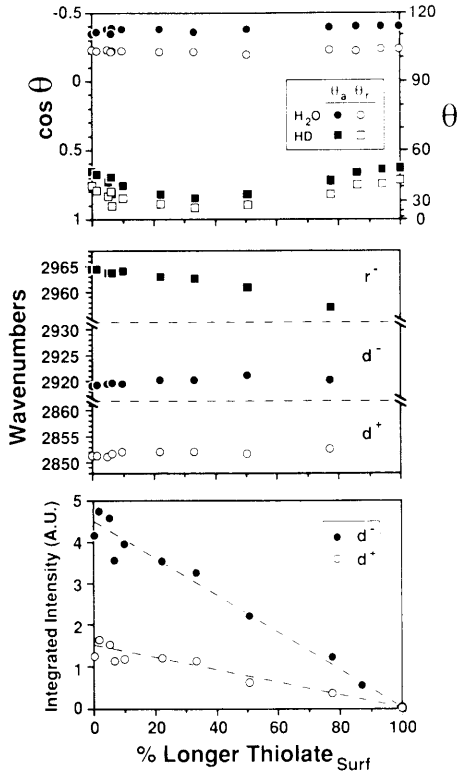

Figure 7. Wetting properties and C–H stretching mode data of SAMs on gold derived from ethanolic solutions containing mixtures of $CH_3(CH_2)_{11}SH$ and $CD_3(CD_2)_{17}SH$. The infrared data are for the shorter *n*-alkylthiolate in the mixed SAMs, namely, those elements of the SAM derived from $CH_3(CH_2)_{11}SH$. The compositions of the SAMs were determined by XPS (see Experimental Section); we estimate the error in surface compositions to be ±5% of the *x*-axis. The dashed lines in the lowest panel are linear least-squares analyses of the data and illustrate that the intensity of methylene modes for the shorter thiolate are linearly related to its composition in the SAM. AU = arbitrary units.

mixed SAM is low and remains constant over all compositions of the SAM. The integrated intensities of the methylene C–H stretching modes (d^+ and d^-) in this experiment exhibit a linear relation with the concentration of the shorter component in the mixed SAM (Figure 7c). This linear relation suggests that the orientation of this component, when in a mixed SAM, is the same as in a pure SAM. The IR data, taken in total, determine that *the dilution by the longer chained component does not constitute a major perturbation of the local molecular environment of the shorter alkanethiolate.*

As in Figure 4a, the lowest values of θ_a(HD) and θ_r(HD) in the C_{12}/C_{18} system occur when the longer alkanethiolate is a minor component of the mixed SAM (Figure 7a). The spectral characteristics of the shorter thiolate in these SAMs are similar to those of a pure SAM although the position of the r^+ and r^- modes are ~2 cm^{-1} lower than they are in pure SAMs. At lower surface concentrations of the shorter alkanethiolate, the methyl C–H stretching modes broaden and shift further in position (Figures 6 and 7b). Stole and Porter have observed similar shifts and broadening (albeit of greater magnitude) in the methyl C–H stretching frequencies of a methyl-terminated SAM on gold upon transferring it from contact with air to a condensed phase (in their case, water, methanol, and CCl_4).[42] These differences between the spectra of mixed and pure SAMs suggest that the methyl groups of the shorter component in these mixed SAMs are not present at the monolayer/air interface, but are instead in contact with a condensed phase,[43] presumably the hydrocarbon chains of the longer alkanethiol. The detailed structural arguments advanced by Stole and Porter[42] involved perturbations beyond those of simple dielectric screening (i.e., media) effects on band intensities (although these are no doubt important). The consequence of solvent contact in their view was to enhance surface disorder. This interpretation is doubtful, given the now well-accepted view that the ambient surface of these structures presents considerable conformational disorder at room temperature even in the absence of solvent.[11c,13,40,44,45] Indeed, what is more striking about these latter trends in the data is that the "band shifts" of the asymmetric methyl C–H stretching modes more correctly indicate, at least to a considerable degree, a *reweighting* of the relative intensities of the r_a^- and r_b^- contributors.[46] These trends are indistinguishable in both magnitude and direction from those occurring on cooling a single-component SAM below 200 K.[11c,47] To this extent then, the coadsorbed perdeuterated long chain does not constitute significant perturbation of the local molecular environment felt by the shorter chained constituent. This perturbation is one, at least for a significant range of mole fractions in the SAM, that the thermal population of chain end gauche conformers in the shorter chain are quenched by the presence of the longer constituent, a notion consistent with its being "buried" in the matrix formed by the latter. That is, in brief, the chain ends of the shorter chains become *more* ordered by contact with the disordered, projecting ends of the longer chains than they would be in a pure single-component phase. Similarly, in the work of Stole and Porter, the observed effects may reflect *increased* order rather than decreased order for chain ends in contact with solvent (relative to the order characterizing the monolayer/air interface).

Discussion

Kinetic and Thermodynamic Considerations Important to Multicomponent SAMs. It is well-known that *n*-alkanes of dissimilar chain lengths (lengths comparable to those employed here[48]) do not form thermodynamically stable solid solutions.[48-50] Phase separation occurs very rapidly in samples quenched from the melt and involves, in all likelihood, a combination of molecular transport mechanisms. (These mechanisms find only incomplete analogies in SAMs, since longitudinal and lateral diffusion of chains along growing lamellae occur.) We are inclined to believe that the equilibrium state of mixed SAMs comprised of adsorbates of dissimilar chain lengths would consist of phase-separated domains. This conclusion follows from the likely inability of the favorable entropy of dilution to compensate effectively the increased van der Waals interactions experienced by chains in a crystalline domain. We can estimate the enthalpic contribution that drives this phase separation. A first-order approximation, for a phase transition of the sort shown in Figure 1a, would be to weight differentially the group constituent binding enthalpies of the CH_2 groups according to the local characteristics of the environment in which they exist (either crystalline or disordered domains). A reasonable estimate would be to equate this enthalpic difference to a group constituent heat of fusion. As judged from the melting points of the *n*-alkanes, this enthalpy would be of the order of ~0.4 kcal/mol of CH_2.[51] For the case of a SAM composed of C_{12} and C_{22} chains, an approximate driving force of 4 kcal/mol would be available to offset a composition dependent entropy of mixing. We therefore conclude that the structures of the mixed SAMs discussed below are in part metastable, kinetically trapped structures: that is, they are mixtures of components that would tend to phase separate, given appropriate conditions.

There exists increasing experimental evidence from our and others' laboratories (which we do not present in detail here) that suggests that thiols adsorbed on gold do yield approximately kinetic structures.[27,28,52] It is only for the simplest adsorbates (e.g., CH_3SSCH_3 adsorbed on Au(111) in UHV[53]) or for very long exposures that the true thermodynamic end points of the assembly are likely to be approached. For single-component SAMs the main point of concern is the time that is required to achieve rigorously the limiting coverage defined by the preferred $(\sqrt{3}\times\sqrt{3})R30°$ habit of the sulfur ligands on the (111) surface. The significant steric repulsions expected for a chain trying to penetrate a high coverage surface suggests that the approach to equilibrium kinetics could be very slow. Strong pinning of adsorbates at surface defects is also likely to affect the rate at which equilibrium is reached.

The mixed SAMs implicitly raise another interesting and complex notion which has only been casually addressed in earlier work. It is clear that the adsorption process is dynamic; in the

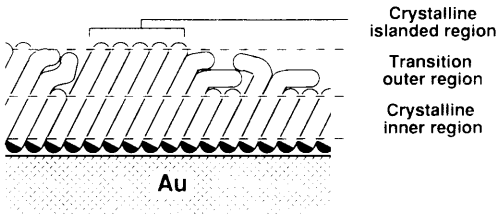

Figure 8. Schematic illustration of the structures present in mixed SAMs on gold derived from competitive adsorption of two *n*-alkanethiols having different chain lengths; see text for spectroscopic arguments.

presence of excess adsorbate, molecules both adsorb and desorb.[6,23,54,55] The latter exchange process is incompletely understood at present but is now thought to involve kinetic exchange processes that are somehow coupled to defects in the overlayer.[6] There is no reason to believe that the processes underlying these exchange phenomena proceed with similar rates for adsorbates of differing molecular structure. It is therefore likely that mixed SAMs could express quantitative structural differences that depend very strongly on the exact details of the sample history.

Structure of the Mixed SAM. The combined weight of the IR data suggests that the shorter alkanethiolate is present in the mixed SAMs, over all surface compositions, in a highly oriented form similar to but differing in some subtle regards from that of a pure SAM (Figures 3b and 6), and that portions of the longer alkanethiolate contain gauche conformers when present in the mixed SAMs (Figure 3a).[56] The strong influence of the coadsorbate on the phase state of the longer chains implicitly argues against the occurrence of a macroscopic phase segregation of the constituents under the preparative conditions employed here. The hydrocarbon chain of the shorter thiolate in the mixed SAMs is like that in a pure C_{12} SAM on gold; namely, it is trans-extended (Figure 7b) and tilted ~27° from the surface normal (Figure 7c). At concentrations of short chains in the SAMs less than ~10%, the perturbation of the methyl mode intensities suggests that the population of chain-end gauche conformers in the shorter chained constituent is in fact lower than that found in the pure SAM at this temperature. The longer thiolate contains high densities of gauche conformers that appear to be localized in specific regions of the adsorbate molecule; their density is a function of the concentration of the longer thiolate in the mixed SAMs (Figure 4b). Given the structure of the shorter alkanethiolate in the mixed SAMs, we infer that the region of the longer chain near the gold must be structurally similar to that of a pure SAM (i.e., trans-extended and canted ~27° from the surface normal) over all surface concentrations, and that the tail (i.e., the portion of the longer alkanethiolate that extends beyond the end of the shorter alkanethiolate) must contain most of the gauche conformers. The band shifts present in the d^+ and d^- modes in Figure 3a are consistent with these structural features. The relative intensities in the d^- and d^+ modes of crystalline (2918 and 2850 cm^{-1}, respectively) and liquidlike regions (~2928 and ~2858 cm^{-1}, respectively) of the longer thiolate, when present as a minor component of the mixed SAM (Figure 3a; $(\% C_{22})_{SAM} < 10\%$), suggest that much of the tail region of the longer thiolate may be in contact with the methyl surface of the shorter alkanethiolate. The spectral changes observed in the r^+ and r^- modes in Figure 6 support the presence of an interaction between the methyl groups of the shorter adsorbate and a condensed phase, presumably the disordered tail of the longer thiolate. At higher surface concentrations of the longer thiolate, the line shapes of the d^- and d^+ modes suggest that the longer thiolate contains a much lower density of gauche conformers than that described immediately above. This decrease may be due to the presence of small clusters of longer thiolates themselves providing for domains of largely trans-extended longer chains; these clusters need not be oriented 27° from the surface normal as would be obtained in a pure SAM. Figure 8 schematically summarizes these structural conclusions.

The general structure that emerges from the IR spectra is one containing a disordered hydrocarbon layer supported on a hydrocarbon underlayer whose structure is similar to and contains comparable molecular orientations as that found in a pure SAM. The IR and wetting data of the mixed SAMs are incompatible with the formation of macroscopic domains each containing one component (Figure 1a): if they had formed, the intensity of methylene C–H stretching modes would be directly related to composition for both components, the density of gauche conformers in each component would be the same as in pure SAMs, no change in the position or width of the peaks assigned to the r^+ and r^- modes would be observed, and the wetting properties would be an appropriately weighted arithmetic sum[57] of those of the pure SAMs. Our data confirm that the two components do not form large islands but do not allow us to distinguish between SAMs that are well-mixed (Figure 1c) or contain small clusters of the same adsorbate (Figure 1b). That the SAMs have a different compositions than the solution from which they were formed suggests that a local preference exists on the surface for the longer alkanethiol and segregation is expected; in these systems, the preference on the surface is for interactions between adsorbates having similar chain lengths (see Figure 2a).[29]

The structure of the exterior region of the mixed SAMs as a function of increasing concentration of the longer thiolate has some similarity to the structures that may be present in monolayers present at air/water interfaces at different surface pressures. Mitchell and Dluhy[58] have observed positions for the d^- mode from 2919 to 2925 cm^{-1} and for d^+ mode from 2850 to 2854 cm^{-1} for monolayer films of 1,2-dipalmitoyl-*sn-glycero*-3-phosphocholine (DPPC) at an air/water interface as its molecular area was varied from 40 to 100 Å^2. Like the data presented in Figure 4b, the position of the d^- and d^+ modes shifted to higher wavenumbers as the molecular concentration of DPPC decreased. The d^- and d^+ modes in the spectra of DPPC did not display the asymmetries exhibited in Figure 3a, consistent with our conclusion that crystalline and liquidlike phases are both present in the longer thiolate of our mixed SAMs.

Relation of Structure to Wetting. The wetting properties of the mixed and pure SAMs are different and must be related to the different structural features present in the mixed SAMs. The interfaces of the mixed SAMs expose a mixture of CH_3 and CH_2 groups, the latter contributing to a higher energy surface,[59] and contain a higher density of gauche conformers than do the pure SAMs; these conformers are concentrated near the monolayer–air(liquid) interface. Wetting is a measure of the interfacial free energy,[60,61] and differences in it between surfaces must reflect differences in the enthalpic and/or entropic interactions of a liquid with the interfaces.

Figures 3 and 6 allow comparison between a macroscopic property of the mixed SAMs, wetting, and microscopic details of their structure. The minimum values of θ_a(HD) occur when the longer alkanethiolate is the minor component of the SAM. Over the range of surface compositions where θ_a(HD) is lowest, the IR spectra define the surface of the mixed SAM to be composed of disordered hydrocarbon chains supported on a crystalline-like hydrocarbon underlayer (Figure 8). For SAMs composed of 20–60% of the longer thiolate, cos θ_a(HD) and cos θ_r(HD) change little. The small change in cos θ_a(HD) and cos θ_r(HD) suggests that the interfacial free energies of these surfaces (γ_{SL}) are similar even though the amount of disorder present in the mixed SAMs, as manifested in the positions of the d^- and d^+ modes, is different. Bain et al. have shown that wetting by HD can be sensitive to the 3-Å region near the surface.[31] The similarity in wetting by HD suggests that this 3-Å region near the surface of the mixed SAMs is similar in composition and degree of disorder over this range of surface compositions. The shifts in the d^- and d^+ modes thus must represent the different amounts of crystalline hydrocarbon domains that are present below this 3-Å region.

The contact angles of water (θ_a and θ_r) are relatively insensitive to the disorder present in the SAMs. The surface of the mixed SAMs should be composed of various amounts of CH_2 and CH_3 groups. The equilibrium (or mean) contact angles of water on surfaces exposing CH_2 groups are reported to be lower than on those exposing CH_3 groups (~105°[62,63] vs 111–115°,[63,64] respectively) and we would expect that the contact angles of water,

in the absence of other effects, would be slightly lower on the mixed SAMs than on the pure SAMs ($\lesssim$6–10°). The only change observed in the contact angles of water is a decrease in θ_r in the C_{12}/C_{22} system (~6°). As this system also exhibits an increased hysteresis in the contact angles of water ($\Delta \cos\theta = \cos\theta_r - \cos\theta_a$), it is difficult to assess whether any of the changes (or lack of changes) in the contact angles of water are controlled by changes in the composition,[57] morphology,[65] or degree of disorder present in the SAMs.

Relation between Hysteresis and Structure. While macroscopic theories exist to explain contact angle hysteresis,[61,65] no microscopic theory is currently available to explain the contact angle hystereses that have been observed in mixed monolayer systems of the type characterized here. Although we realize that the structure of the mixed SAMs may be different when contacted with a condensed phase from that determined (by IR) for the SAM in contact with air (Figures 8 and 9a), some similarities no doubt do exist. Our discussion here is intended to summarize the various data concerning hysteresis in related systems in the literature[28,29] and compare them with the structural elements determined in this paper and in related systems.

As in previous studies,[28,29] we observed increased hysteresis in the contact angles of water on mixed SAMs on gold derived from $C_{12}SH$ and $C_{22}SH$ relative to the pure SAMs (Figure 2). Smaller increases in hysteresis have been observed[28] with mixed SAMs composed of adsorbates having smaller differences in the chain lengths of the two adsorbates and are consistent with our observation here that little change in hysteresis occurred in the C_{12}/C_{18} system (Figure 5). Bain et al.[28] have observed in similar mixed systems that, while the hystereses in the contact angles of *n*-alkanes (HD and decane) do not change with surface composition, the hysteresis in the contact angles of bicyclohexyl and water do. The maximum hystereses of water and bicyclohexyl consistently occurred when the SAMs had an equimolar composition of the longer and shorter thiolates.

From the data presented here, SAMs having equimolar compositions consist of shorter thiolates that are present in an oriented, largely trans-extended form, and of longer thiolates that contain gauche conformers. The apparent weighted per chain density of gauche conformers in the longer thiolate, as manifested in the positions of the peak maxima of the d^- and d^+ modes, is lower in the SAMs that contain a 1:1 composition of the two thiolates than in those that contain lower concentrations of the longer thiolate (Figure 4b). In Figure 4c, for ratios of the two components ranging from 2:1 to 1:2, the largest deviations in the intensities of these modes from those expected for thiolates in a crystalline form oriented 27° from the surface normal are observed. As the 27° cant angle results from dense packing of the hydrocarbon chains on the $(\sqrt{3}\times\sqrt{3})R30°$ lattice on gold,[36] these deviations suggest that many of the hydrocarbon chains at the surface are not as densely packed. The range of surface compositions where a maximum amount of hydrocarbon chains is not present in a densely packed fashion occurs over the same range where the hystereses in the contact angles of water and bicyclohexyl are at a maximum. This correspondence suggests that hysteresis between dissimilar phases may be determined by amounts of molecular-level structural heterogeneity and possibly roughness.[66] Although the exact details of the structure of mixed SAMs when contacting these liquids are unclear, we expect that, based the immiscibility of alkanes and water, contact with water would only modestly perturb the structure of the mixed SAMs from that determined for them by IR (Figure 9a).

Over this intermediate range of surface compositions (2:1 to 1:2), the hystereses in the contact angles of HD and decane exhibit little change (Figures 2 and 5, and refs 28 and 29) and we can only presume that the similarities between the structure and chemical nature of the SAM and of the contacting liquids are responsible. The exact structure of the mixed SAMs, when in contact with HD or decane, is one probably restructured to some degree by these liquids (Figure 9b). The exterior region of the SAMs, when in contact with these liquids, may therefore bear little resemblance to that pictured in Figure 8. The internal,

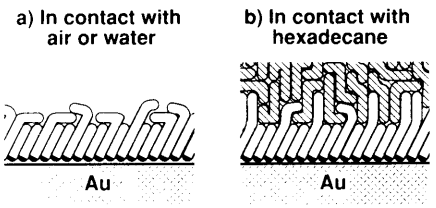

Figure 9. Schematic illustration of the different structures that may be present when the mixed SAMs on gold are contacted with different phases.

crystalline region of the SAM, however, should be affected little by solvent and is probably similar in structure to Figure 8.

In a limited way, these mixed SAMs are analogous to binary mixtures of shorter and longer *n*-alkanes. In these systems, Snyder et al. have observed that the conformational disorder of the longer *n*-alkane reached a maximum for mixtures of ~1:1 composition.[48,50] The level of conformational disorder in the longer *n*-alkane was greater when the difference in chain length between the two alkanes was greater.[50] The observations noted here that the hystereses in the contact angles of water and bicyclohexyl reach maxima when the surface composition is ~1:1,[67] and that the observed hystereses are lower when the difference between the chain lengths of the adsorbates is reduced strongly suggest that the hystereses in the contact angles of water and bicyclohexyl are sensitive to the presence of conformational disorder. By analogy, hexadecane and decane are not sensitive to this disorder.

Conclusions

Mixed monolayers obtained by adsorption of alkanethiols having different chain lengths on gold contain specific regions of order and disorder; the region closest to the gold contains a much lower density of gauche conformers than the region closer to the monolayer/air interface. The highest weighted per chain density of gauche conformers is observed in the longer alkanethiolate when its surface composition is low; the greatest amount of disorder in the longer alkanethiolate is observed in SAMs having approximately equimolar composition. The interplay between entropic and enthalpic contributions to the interfacial free energy of the SAMs is manifested differently in the wetting properties of water and hexadecane: the contact angles of hexadecane are more sensitive to the *density* of conformational disorder present in the longer *n*-alkanethiolate than those of water are; the hysteresis in $\theta(H_2O)$ is more sensitive to the *amount* of conformational disorder present in the longer *n*-alkanethiolate than the hysteresis in θ(HD).

Experimental Section

Materials. Dodecane- and docosanethiol were available from previous studies.[23] 1-Bromooctadecane-d_{37} and 1-bromododecane-d_{25} were obtained from Cambridge Isotopes Laboratories (98% D); thiolacetic acid was from Aldrich. Dioxygen was removed from absolute EtOH (Quantum Chemical Corp., Tuscola, IL) by bubbling N_2 through it prior to use. Si(100) wafers (test grade; 50 and 100 mm), Au (99.999%) and Cr (99.997%) were obtained from Silicon Sense (Nashua, NH), Materials Research Corp. (Orangeburg, NY), and Aesar, respectively.

***n*-$C_{12}D_{25}SH$ and *n*-$C_{18}D_{37}SH$.** The thiols were prepared from the corresponding bromides by displacement with sodium thioacetate and subsequent acidic methanolysis.[23] The alkyl thioacetates and thiols were purified by column chromatography (silica gel) and exhibited the same values of R_f as authentic samples not containing deuteriums. SAMs derived from adsorption of these thiols had indistinguishable properties by wetting, ellipsometry, and XPS from those prepared from pure samples of $C_{12}H_{25}SH$ and $C_{18}H_{37}SH$, respectively.

Preparation and Characterization of Monolayers. Evaporated films of Au (2000 Å) were prepared onto Cr-primed Si(100) wafer as previously described.[20] SAMs were formed by exposing the Au films to ethanolic solutions containing mixtures of the two alkanethiols for 24–48 h. The SAMs were removed from solution and rinsed with EtOH prior to characterization. Ellipsometric

constants were measured using a Rudolph Research Type 43603-200E ellipsometer (He–Ne laser at an incident angle of 70°) before and after immersion of the gold substrate in the contacting solution; thicknesses were calculated using a parallel, homogeneous, three-layer model[68] and a refractive index of 1.45.[11a,23,29] Advancing and receding contact angles were measured using a Ramé-Hart Model 100 goniometer on static drops (syringe tip attached to the drop) that were applied/re-treated using a Matrix Technologies Electra-pipette (~1 μL/s). Data in the figures represent the average of at least three measurements of the contact angles on both sides of the drop. X-ray photoelectron spectra were obtained on a Surface Science X-100 XPS spectrometer using a monochromatized Al Kα source (beam diameter = 1000 μm) and a pass energy of 100 eV at a take-off angle of 35° from the surface parallel. Acquisition times for C(1s) and Au(4f) spectra were <5 min each; X-ray-induced damage to the SAM was negligible on these time scales.[69] Spectra were fitted using Shirley backgrounds[70] and symmetrical 70% Gaussian/30% Lorentzian profiles. Film thicknesses were calculated using the attenuation of the Au(4f) signal through the SAM[71] or from the ratio of the C(1s) and Au(4f) signals.[55] PIERS spectra were obtained as previously described.[11b]

Acknowledgment. We are grateful to Colin D. Bain and John P. Folkers for valuable discussions and suggestions.

Registry No. $C_{12}SH$, 112-55-0; $C_{18}SH$, 2885-00-9; $C_{22}SH$, 7773-83-3; Au, 7440-57-5; hexadecane, 544-76-3.

References and Notes

(1) This research was supported in part by the Office of Naval Research and by the National Science Foundation (Grant CHE-88-12709). XPS spectra were obtained using instrumental facilities purchased under the DARPA/URI program and maintained by the Harvard University Materials Research Laboratory. R.G.N. acknowledges support from the Department of Energy through the UIUC-MRL (DEFG02-91ER 45439).

(2) (a) Bain, C. D.; Evall, J.; Whitesides, G. M. *J. Am. Chem. Soc.* **1989**, *111*, 7155–7164. (b) Laibinis, P. E.; Whitesides, G. M. *J. Am. Chem. Soc.* **1992**, *114*, 1990–1995.

(3) Ulman, A.; Evans, S. D.; Shnidman, Y.; Sharma, R.; Eilers, J. E.; Chang, J. C. *J. Am. Chem. Soc.* **1991**, *113*, 1499–1506.

(4) Pale-Grosdemange, C.; Simon, E. S.; Prime, K. L.; Whitesides, G. M. *J. Am. Chem. Soc.* **1991**, *113*, 13–20.

(5) (a) Häussling, L.; Michel, B.; Ringsdorf, H.; Rohrer, H. *Angew. Chem., Int. Ed. Engl.* **1991**, *30*, 569–572. (b) Prime, K. L.; Whitesides, G. M. *Science (Washington, D.C.)* **1991**, *252*, 1164–1167. (c) Prime, K. L.; Whitesides, G. M. Manuscript in preparation.

(6) (a) Chidsey, C. E. D.; Bertozzi, C. R.; Putvinski, T. M.; Mujsce, A. M. *J. Am. Chem. Soc.* **1990**, *112*, 4301–4306. (b) Chidsey, C. E. D. *Science (Washington, D.C.)* **1991**, *251*, 919–922.

(7) Rowe, G. K.; Creager, S. E. *Langmuir* **1991**, *7*, 2307–2312.

(8) Hickman, J. J.; Ofer, D.; Laibinis, P. E.; Whitesides, G. M.; Wrighton, M. S. *Science (Washington, D.C.)* **1991**, *252*, 688–691.

(9) Swalen, J. D.; Allara, D. L.; Andrade, J. D.; Chandross, E. A.; Garoff, S.; Israelachvili, J.; McCarthy, T. J.; Murray, R.; Pease, R. F.; Rabolt, J. F.; Wynne, K. J.; Yu, H. *Langmuir* **1987**, *3*, 932–950.

(10) Sum-frequency spectroscopy: (a) Harris, A. L.; Chidsey, C. E. D.; Levinos, N. J.; Loiacono, D. N. *Chem. Phys. Lett.* **1987**, *141*, 350–356. (b) Bain, C. D.; Davies, P. B.; Ong, T. H.; Ward, R. N.; Brown, M. A. *Langmuir* **1991**, *7*, 1563–1566.

(11) IR spectroscopy: (a) Porter, M. D.; Bright, T. B.; Allara, D. L.; Chidsey, C. E. D. *J. Am. Chem. Soc.* **1987**, *109*, 3559–3568. (b) Nuzzo, R. G.; Dubois, L. H.; Allara, D. L. *J. Am. Chem. Soc.* **1990**, *112*, 558–569. (c) Nuzzo, R. G.; Korenic, E. M.; Dubois, L. H. *J. Chem. Phys.* **1990**, *93*, 767–773. (d) Reference 20. (e) Evans, S. D.; Urankar, E.; Ulman, A.; Ferris, N. *J. Am. Chem. Soc.* **1991**, *113*, 4121–4131. (f) Evans, S. D.; Goppert-Berarducci, K. E.; Urankar, E.; Gerenser, L. J.; Ulman, A.; Snyder, R. G. *Langmuir* **1991**, *7*, 2700–2709.

(12) Transmission electron microscopy (TEM): Strong, L.; Whitesides, G. M. *Langmuir* **1988**, *4*, 546–558; for a reanalysis of some of the data in this paper, see: Chidsey, C. E. D.; Loiacono, D. N. *Langmuir* **1990**, *6*, 682–691.

(13) Low-energy helium diffraction: (a) Chidsey, C. E. D.; Liu, G.-Y.; Rowntree, P.; Scoles, G. *J. Chem. Phys.* **1989**, *91*, 4421–4423. (b) Camillone III, N.; Chidsey, C. E. D.; Liu, G.-Y.; Putvinski, T. M.; Scoles, G. *J. Chem. Phys.* **1991**, *94*, 8493–8502.

(14) X-ray diffraction: Samant, M. G.; Brown, C. A.; Gordon III, J. G. *Langmuir* **1991**, *7*, 437–439; using the same technique, Fenter et al.[21e] obtained a different value of the cant angle (~30° vs surface normal) than Samant et al. reported (~10°).

(15) Scanning tunneling microscopy (STM): Widrig, C. A.; Alves, C. A.; Porter, M. D. *J. Am. Chem. Soc.* **1991**, *113*, 2805–2810.

(16) Raman spectroscopy: Bryant, M. A.; Pemberton, J. E. *J. Am. Chem. Soc.* **1991**, *113*, 8284–8293.

(17) *n*-Alkanoic acids on Al_2O_3. IR spectroscopy: Allara, D. L.; Nuzzo, R. G. *Langmuir* **1985**, *1*, 52–66.

(18) α,ω-Alkanedicarboxylic acids on Ag_2O. IR spectroscopy: Allara, D. L.; Atre, S. V.; Elliger, C. A.; Snyder, R. G. *J. Am. Chem. Soc.* **1991**, *113*, 1852–1854.

(19) *n*-Alkyltrichlorosilanes on SiO_2. IR spectroscopy: (a) Tillman, N.; Ulman, A.; Schildkraut, J. S.; Penner, T. L. *J. Am. Chem. Soc.* **1988**, *110*, 6136–6144. (b) Tillman, N.; Ulman, A.; Elman, J. F. *Langmuir* **1989**, *5*, 1020–1026. X-ray reflectivity and diffraction: (c) Wasserman, S. R.; Whitesides, G. M.; Tidswell, I. M.; Ocko, B. M.; Pershan, P. S.; Axe, J. D. *J. Am. Chem. Soc.* **1989**, *111*, 5852–5861. (d) Daillant, J.; Benattar, J. J.; Léger, L. *Phys. Rev. A* **1990**, *41*, 1963–1977. (e) Tidswell, I. M.; Rabedeau, T. A.; Pershan, P. S.; Kosowsky, S. D.; Folkers, J. P.; Whitesides, G. M. *J. Chem. Phys.* **1991**, *95*, 2854–2861.

(20) *n*-Alkanethiols on Cu. IR spectroscopy: Laibinis, P. E.; Whitesides, G. M.; Allara, D. L.; Tao, Y.-T.; Parikh, A. N.; Nuzzo, R. G. *J. Am. Chem. Soc.* **1991**, *113*, 7152–7167.

(21) *n*-Alkanethiols on Ag. IR spectroscopy: (a) Walczak, M. W.; Chung, C.; Stole, S. M.; Widrig, C. A.; Porter, M. D. *J. Am. Chem. Soc.* **1991**, *113*, 2370–2378. (b) Reference 20. Raman spectroscopy: (c) Bryant, M. A.; Pemberton, J. E. *J. Am. Chem. Soc.* **1991**, *113*, 3629–3637. Sum-frequency spectroscopy: (d) Reference 10b. X-ray diffraction and low-energy helium diffraction: (e) Fenter, P.; Eisenberger, P.; Li, J.; Camillone III, N.; Bernasek, J.; Scoles, G.; Ramanarayanan, T. A.; Liang, K. S. *Langmuir* **1991**, *7*, 2013–2016.

(22) Nuzzo, R. G.; Allara, D. L. *J. Am. Chem. Soc.* **1983**, *105*, 4481–4483.

(23) Bain, C. D.; Troughton, E. B.; Tao, Y.-T.; Evall, J.; Whitesides, G. M.; Nuzzo, R. G. *J. Am. Chem. Soc.* **1989**, *111*, 321–335.

(24) Nuzzo, R. G.; Fusco, F. A.; Allara, D. L. *J. Am. Chem. Soc.* **1987**, *107*, 2358–2368.

(25) For reviews, see: (a) Bain, C. D.; Whitesides, G. M. *Angew. Chem., Int. Ed. Engl.* **1989**, *101*, 522–528. (b) Whitesides, G. M.; Laibinis, P. E. *Langmuir* **1990**, *6*, 87–96.

(26) For SEM and STM images of the Au surfaces used in these studies, see ref 29.

(27) (a) Bain, C. D.; Whitesides, G. M. *Science (Washington, D.C.)* **1988**, *240*, 62–63. (b) Bain, C. D.; Whitesides, G. M. *J. Am. Chem. Soc.* **1988**, *110*, 3665–3666. (c) Folkers, J. P.; Laibinis, P. E.; Whitesides, G. M. *J. Adhes. Sci. Technol.*, submitted for publication.

(28) Bain, C. D.; Whitesides, G. M. *J. Am. Chem. Soc.* **1989**, *111*, 7164–7175.

(29) Folkers, J. P.; Laibinis, P. E.; Whitesides, G. M. *Langmuir*, in press.

(30) Hugh, D. R. *Adv. Colloid Interface Sci.* **1980**, *14*, 3–41.

(31) Bain, C. D.; Whitesides, G. M. *J. Am. Chem. Soc.* **1988**, *110*, 5897–5898.

(32) Wilson, M. D.; Ferguson, G. S.; Whitesides, G. M. *J. Am. Chem. Soc.* **1990**, *112*, 1244–1245.

(33) The structures outlined schematically in Figure 1 present an interesting variety of characteristics which do not fit easily into the conventional notions used to describe ordering in condensed-phase systems. As we have noted above, all the SAMs with which this study is concerned are "ordered", at least as judged by the epitaxial arrangements adopted by the sulfur ligands on the Au(111) lattice plane (i.e., $(\sqrt{3}\times\sqrt{3})R30°$). The phase diagram of the hydrocarbon chains is, however, complex. To describe the structural features of this portion of the SAM, it is useful to employ qualitative definitions of the term "ordered" and "crystalline". In the best-defined single-component SAMs, ones in which ordering has been rigorously demonstrated by diffraction,[12,14] the correlation lengths are typically modest (60–70 Å). This aspect of chain structure is likely to be strongly influenced by the coadsorption of chains of differing lengths, a feature central to the current studies. The important qualitative notions which emerge from a consideration of the simplified structures depicted in Figure 1 are ones that are centered on the conformational states adopted by the chains. To the extent that ordered phases are typically ones containing few gauche conformations, we employ the term "crystalline" to describe the character of similar domains present in the SAM. The use of this word does not imply the rigorous long-range positional correlations typically associated with crystalline solids. Any claim of long-range, low-defect order can come only from careful diffraction studies. In the present context, unless explicitly indicated, "crystalline" is only meant to define a local microchemical environment for the chains (or portion thereof) which is similar to that found in the bulk, ordered (crystalline) phases of, for example, *n*-alkanes.

(34) While diffraction methods are extremely powerful in defining order, IR spectroscopy is superior to them in distinguishing between degrees of disorder.

(35) (a) Bunn, C. W. *Trans. Faraday Soc.* **1939**, *35*, 482–491. (b) Shearer, H. M. M.; Vand, V. *Acta Cryst.* **1956**, *9*, 379–384. (c) Wunderlich, B. *Macromolecular Physics Vol. 1*; Academic Press: New York, 1973; p 97.

(36) Bareman, J. P.; Klein, M. L. *J. Phys. Chem.* **1990**, *94*, 5202–5205.

(37) Snyder, R. G.; Hsu, S. L.; Krimm, S. *Spectrochim. Acta, Part A* **1978**, *34*, 395–406.

(38) MacPhail, R. A.; Strauss, H. L.; Snyder, R. G.; Elliger, C. A. *J. Phys. Chem.* **1984**, *88*, 334–341.

(39) The intensity of the IR modes is a function ($I/I_0 = 3\cos^2\phi_{mz}$) of the orientation (ϕ_{mz}) of the vector of the dipole moment relative to the surface normal. I_0 is the intensity of the mode in an anisotropic material. For an illustration of how changes in ϕ_{mz} can affect the IR spectra of *n*-alkylthiolate SAMs, see ref 20.

(40) Hautman, J.; Klein, M. L. *J. Chem. Phys.* **1989**, *91*, 4994–5001.

(41) From Figures 3b and 6, the intensity of the C–D stretching modes (d^+ and d^-) of a perdeuterated C_{12} SAM is ~40% the intensity of the C–H stretching modes for a perprotonated C_{12} SAM. This reduced intensity limits our ability to assess reliably the magnitude of band shifts that occur at low mole fractions of the perdeuterated C_{12} component given the baseline artifacts that we observe in this spectral region.

(42) Stole, S. M.; Porter, M. D. *Langmuir* **1990**, *6*, 1199–1202.

(43) (a) Caldow, G. L.; Cunliffe-Jones, D.; Thompson, H. W. *Proc. R. Soc. London, A* **1959**, *254*, 17–29. (b) Buckingham, A. D. *Proc. R. Soc. London, A* **1960**, *255*, 32–39. (c) Pullin, A. D. E. *Proc. R. Soc. London, A* **1960**, *255*, 39–43.

(44) Diffraction studies have shown that the density of gauche conformers at the methyl/vapor(vacuum) interface, even at much lower temperatures (~35 K), is greater than the density present in the bulk of a SAM at room temperature: domain sizes for the methyl surfaces of various SAMs are 26–44 Å at ~35 K;[13] the domain size for the SAM is 60–70 Å at ~300 K.[12,14]

(45) For examples in related systems, see: (a) Barton, S. W.; Thomas, B. N.; Flom, E. B.; Rice, S. A.; Lin, B.; Peng, J. B.; Ketterson, J. B.; Dutta, P. *J. Chem. Phys.* **1988**, *89*, 2257–2270. (b) Harris, J.; Rice, S. A. *J. Chem. Phys.* **1988**, *89*, 5898–5908.

(46) The reweighting of the r_a^- and r_b^- contributors is most evident in the IR spectra in Figure 6 for mixed SAMs derived from solutions having ratios of the two components ($[C_{12}]_{soln}/[C_{18}]_{soln}$) of 4 and 6. For these mixed SAMs, the r^- spectral envelopes are significantly broader than for those of pure SAMs and their "peaks" occur at wavenumbers lower than that for the pure SAM. These features can be readily explained by an increase in the relative intensity of the r_b^- contributor (see ref 47). The result of this reweighting is that the r^- spectral envelope in these spectra appear broader than those of a pure SAM and have maximum intensity at frequencies between those associated with the r_a^- and r_b^- modes (Table I).

(47) As the thermal population of gauche conformers are quenched in an *n*-alkanethiolate SAM on gold, the absolute (and relative) intensity (I) of the r_b^- mode has been shown to increase: at 300 K, $I(r_b^-)/I(r_a^-) \approx 0.4$; at 150 K, $I(r_b^-)/I(r_a^-) \approx 1$.[11c]

(48) Maroncelli, M.; Strauss, H. L.; Snyder, R. G. *J. Phys. Chem.* **1985**, *89*, 5260–5267.

(49) Mnyukh, Y. V. *J. Struct. Chem. (USSR)* **1960**, *1*, 346–365.

(50) Kim, Y.; Strauss, H. L.; Snyder, R. G. *J. Phys. Chem.* **1989**, *93*, 485–490.

(51) Broadhurst, M. G. *J. Res. Natl. Bur. Stand., A* **1962**, *66*, 241–249.

(52) (a) Folkers, J. P.; Laibinis, P. E.; Whitesides, G. M. Manuscript in preparation. (b) Biebuyck, H. A.; Whitesides, G. M. Unpublished results.

(53) Nuzzo, R. G.; Zegarski, B. R.; Dubois, L. H. *J. Am. Chem. Soc.* **1987**, *109*, 733–740.

(54) (a) Hickman, J. J.; Ofer, D.; Zou, C. F.; Wrighton, M. S.; Laibinis, P. E.; Whitesides, G. M. *J. Am. Chem. Soc.* **1991**, *113*, 1128–1132. (b) Collard, D. M.; Fox, M. A. *Langmuir* **1991**, *7*, 1192–1197. (c) Biebuyck, H. A.; Whitesides, G. M. Unpublished results.

(55) Laibinis, P. E.; Fox, M. A.; Folkers, J. P.; Whitesides, G. M. *Langmuir* **1991**, *7*, 3167–3172.

(56) Similar results have been observed in binary solid solutions of *n*-$C_{19}H_{40}$ and *n*-$C_{21}H_{44}$: the concentration of gauche conformations in the ends of the longer *n*-alkane monotonically decreased as its concentration in the mixture was increased; the concentration of gauche conformers in the ends of the shorter *n*-alkane changed relatively little with composition.[48]

(57) (a) Cassie, A. B. D. *Discuss. Faraday Soc.* **1948**, *3*, 11–16. (b) Israelachvili, J. N.; Gee, M. L. *Langmuir* **1989**, *5*, 288–289.

(58) Mitchell, M. L.; Dluhy, R. A. *J. Am. Chem. Soc.* **1988**, *110*, 712–718.

(59) The critical surface tensions (γ_c) of CH_3 and CH_2 surfaces are 22–24 and 31 dyn/cm, respectively (Shafrin, E. G.; Zisman, W. A. *J. Phys. Chem.* **1960**, *64*, 519–524).

(60) Young's equation ($\cos\theta_e = (\gamma_{SV} - \gamma_{SL})/\gamma_{LV}$) relates the equilibrium contact angle (θ_e) to the free energies (γ) of the solid–liquid–vapor (S–L–V) interfaces (Young, T. *Philos. Trans. R. Soc. (London)* **1805**, *95*, 65–87).

(61) de Gennes, P. G. *Rev. Mod. Phys.* **1985**, *57*, 827–863.

(62) Adam, N. K.; Elliott, G. E. P. *J. Chem. Soc.* **1962**, 2206–2209.

(63) Spelt, J. K.; Neumann, A. W. *Langmuir* **1987**, *3*, 588–591.

(64) Fox, H. W.; Zisman, W. A. *J. Colloid Sci.* **1950**, *5*, 428–442.

(65) (a) Wenzel, R. N. *Ind. Eng. Chem.* **1936**, *28*, 988–994. (b) Johnson, Jr., R. E.; Dettre, R. H. In *Contact Angle, Wettability, and Adhesion*; Gould, R. F., Ed.; Advances in Chemistry 43; American Chemical Society: Washington, DC, 1964; Chapter 7. (c) Dettre, R. H.; Johnson, Jr., R. E. In *Contact Angle, Wettability, and Adhesion*; Gould, R. F., Ed.; Advances in Chemistry 43; American Chemical Society: Washington, DC, 1964; Chapter 8. (d) Joanny, J. F.; de Gennes, P. G. *J. Chem. Phys.* **1984**, *81*, 552–562. (e) Schwartz, L. W.; Garoff, S. *Langmuir* **1985**, *1*, 219–230.

(66) The different hystereses that are observed in the contact angles of water on the mixed SAMs are not due to the chemical heterogeneity of the interfaces (CH_2 and CH_3 groups). In other studies,[2b] we have shown that the hysteresis in wetting on SAMs derived from mixtures of $HS(CH_2)_nX$ and $HS(CH_2)_nY$ by water remains constant over all compositions of the SAM.

(67) As a function of composition, both the hysteresis in the contact angles of water on the mixed *n*-alkanethiolate SAMs[29] and the amount of conformational disorder present in binary solid solutions of *n*-alkanes[50] have similar functional forms: minima occur for pure samples and broad maxima occur over a range of intermediate compositions (2:1 to 1:2).

(68) McCrackin, F. L.; Passaglia, E.; Stromberg, R. R.; Steinberg, H. L. *J. Res. Natl. Bur. Stand., A* **1963**, *67*, 363–377.

(69) Laibinis, P. E.; Graham, R. L.; Biebuyck, H. A.; Whitesides, G. M. *Science (Washington, D.C.)* **1991**, *254*, 981–983.

(70) Shirley, D. A. *Phys. Rev. B* **1972**, *5*, 4709–4714.

(71) (a) Bain, C. D.; Whitesides, G. M. *J. Phys. Chem.* **1989**, *93*, 1670–1673. (b) Laibinis, P. E.; Bain, C. D.; Whitesides, G. M. *J. Phys. Chem.* **1991**, *95*, 7417–7421.